

Bulk and interfacial liquid water as a transient network

Miriam Jahn and Stephan Gekle*

Fachbereich Physik, Universität Bayreuth, Germany

(Received 2 September 2015; revised manuscript received 23 October 2015; published 20 November 2015)

The special macroscopic properties of liquid water stem from its structure as a complex network of molecules connected by hydrogen bonds. While the dynamics of single molecules within this network has been extensively investigated, only little attention has been paid to the closed loops (meshes) of hydrogen-bonded molecules which determine the network topology. Using molecular dynamics simulations we analyze the size, shape, geometrical arrangement, and dynamical stability of loops containing up to 10 hydrogen bonds. We find that six-membered loops in liquid water even at room temperature retain a striking similarity with the well-known structure of ice. Analyzing the network dynamics we find that rings of more than five hydrogen bonds are stabilized compared to a random collection containing the same number of single bonds. We finally show that in the vicinity of hydrophobic and hydrophilic interfaces loops arrange in a preferred orientation.

DOI: [10.1103/PhysRevE.92.052130](https://doi.org/10.1103/PhysRevE.92.052130)

PACS number(s): 61.20.Ja, 61.20.Ne, 87.10.Tf, 68.08.De

I. INTRODUCTION

The structure and dynamics of liquid water have always been a subject of intense scientific research and debate. Renewed interest in this field has arisen over the last few years due to the growing awareness that water in many biological processes is much “more than a bystander” [1,2] and that the water structure and dynamics are an essential ingredient for the proper functioning of living organisms. While the notion of liquid water as a “hydrogen bond network” is well established and often repeated, many experimental, computational, and theoretical works focus on the dynamics of a single molecule or a single hydrogen bond connecting two molecules. Examples include investigations of molecular diffusion [3–5] and rotation [6–14], molecular coordination and ordering near interfaces [15–18], or studies on the optimal definition [19–24] and life time [25–29] of the hydrogen bond itself. Collective effects have been studied in terms of wave-vector-dependent scattering functions [30–32] or in the context of dielectric properties in bulk [33–36] and near interfaces [17,37–41] which under certain conditions can be related to nonlocal theories [42–44].

Yet surprisingly little effort has been dedicated to the investigation of the actual characteristics of liquid water from the viewpoint of a true transient network. Almost the only thing that is known in this respect is the fact that the most frequently occurring loop size contains six hydrogen-bonded molecules [19,20,45–47], which has been speculated to be a remnant of the ice Ih structure [46].

Here we use molecular dynamics simulations to investigate the structure and dynamics of liquid water as a transient network, both in bulk and at model interfaces. We first show that the form and arrangement of six-fold meshes in liquid water is very similar to that in ice. Analyzing the dynamics we find that loops of five and six molecules experience some stabilization compared to random groups with the same size. Larger loops are increasingly destroyed by short-circuiting, but the participating hydrogen bonds form an intact ring for

an unexpectedly long period. The last part is devoted to the influence of interfaces on the network topology and dynamics.

II. METHODS

We analyze classical molecular dynamics (MD) simulations of SPC/E water molecules [48]. Simulations are run using GROMACS [49] and the force field GROMOS 53A6 [50]. All simulations are performed in the NVT-ensemble at room temperature using the Nosé-Hoover thermostat. The long-range electrostatics are handled with the smooth Particle-Mesh-Ewald method [51]. The van der Waals potential and the Coulomb potential are switched at 1.0 nm and 1.2 nm, respectively. The OH-bond length is kept constant at 0.1 nm using the SETTLE algorithm [52].

When analyzing the influence of interfaces we confine the water in the z direction by two diamond sheets as described in Refs. [53–55]. The hydrophobic interface is terminated with hydrogen atoms. For a hydrophilic interface 25% of the terminating hydrogens are replaced by hydroxyl groups.

To decide whether two molecules share a hydrogen bond we use the geometric definition of Luzar and Chandler [25]. According to this definition a hydrogen bond between two water molecules exists when the oxygen-oxygen distance is less than 0.35 nm and the angle between the O-O axis and one O-H axis of the molecules is smaller than 30° [Fig. 1(a)]. Simple geometric definitions have proved to be reliable [20], however, the optimal definition of hydrogen bonds is still subject to current research [23,24].

To analyze the shape and orientation of loops we need to find the best fitting plane to which the sum of the squared distances of the N molecules at positions \vec{p}_i is minimal:

$$\chi^2 = \sum_{i=1}^N \frac{|(\vec{p}_i - \vec{p}_0) \cdot \vec{n}|^2}{|\vec{n}|^2} \stackrel{!}{=} \min, \quad (1)$$

where \vec{n} is the normal vector and \vec{p}_0 is one point in the plane of interest, e.g., the center of the loop. The total least-squares problem of finding \vec{n} can be rewritten in matrix form:

$$\chi^2(\vec{n}) = \frac{\vec{n} \cdot (\mathbf{M}^T \mathbf{M}) \cdot \vec{n}}{n^2} \stackrel{!}{=} \min \quad (2)$$

*Stephan.Gekle@uni-bayreuth.de

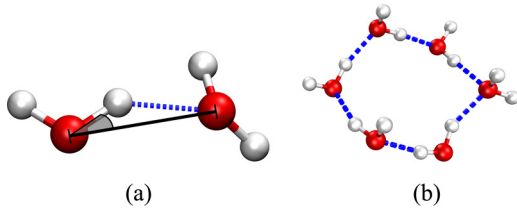


FIG. 1. (Color online) (a) Geometric definition of a hydrogen bond. (b) A loop of six hydrogen-bonded water molecules.

with

$$\mathbf{M} = \begin{pmatrix} x_1 - x_0 & y_1 - y_0 & z_1 - z_0 \\ \dots & \dots & \dots \\ x_N - x_0 & y_N - y_0 & z_N - z_0 \end{pmatrix}. \quad (3)$$

Equation (2) is the Rayleigh quotient, which is known to be minimal for $\vec{n} = \vec{v}_{\min}$, the eigenvector corresponding to the smallest eigenvalue of the matrix $\mathbf{M}^T \mathbf{M}$. The problem of finding this eigenvector is numerically best solved by singular value decomposition [56] of the matrix \mathbf{M} , which directly yields all three principal axes of inertia.

III. RESULTS

A. Network topology in bulk water

In this work we focus on the investigation of the loops that make up the hydrogen-bond network. We define a *loop* as a closed path of hydrogen bonds that is not short-circuited [Fig. 1(b)]; i.e., the shortest path connecting each pair of water molecules is along the loop. Below we will define a *ring* as a closed path of hydrogen bonds which, in contrast to the loop, allows short-circuiting. Accordingly, the occurrence of very large loops becomes increasingly unlikely as there will almost always be a shortcut between two members. The number of rings of a certain size, however, increases the larger the ring size is chosen, limited only by the finite size of the sample.

Independent of the water model and hydrogen-bond definition, five to seven-membered loops have been found to occur most frequently in bulk water [19,20,45–47]. This finding has been speculated to be a remnant of the natural crystal structure of frozen water (ice Ih), which contains hexagonal loops only. N molecules arranged in such a perfect (periodic) ice crystal form $2N$ six-membered loops, whereas our results confirm earlier studies finding that in liquid water fewer than $0.3N$ six-membered loops remain (Fig. 2). Loops with more than 10 members are rather unlikely to occur and are therefore not considered further. While the occurrence of loops has recurrently been cited as an indicator of the true network structure of water, their shape and arrangement has thus far not been analyzed to reveal the actual topology of this network.

The shape of a loop is determined by the positions of the involved molecules. To maintain the hydrogen bonds every molecule needs to stay in a certain angular and distance range relative to its nearest neighbors (cf. Fig. 1). Even within these limits, however, plenty of different and truly three-dimensional configurations of the molecules in a given loop are conceivable.

Nevertheless, we find that the actually realized loop shapes are quite planar. We arrive at this result by measuring the deviation of the molecule positions along the principal axes

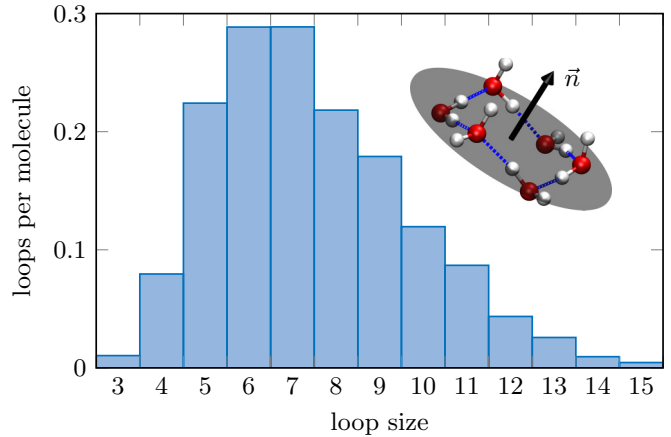


FIG. 2. (Color online) Six- and seven-membered loops occur most frequently in bulk water. Inset: A typical six-membered loop has an almost planar shape, which can be approximated by the plane indicated by the gray disk.

of inertia of the loop (which are calculated as detailed in the Methods section). A six-membered loop in bulk water, for example, has an average height of 0.18 nm occupying a base area of 0.48 nm:0.56 nm. In ice these loops fit into a slightly smaller and flatter cuboid with 0.11 nm:0.46 nm:0.50 nm edge length. A similar result is obtained for all loop sizes between 4 and 10 members, which each fit into a flat cuboid whose height is less than half the length of the other edges.

To obtain a more detailed description of the geometric arrangement of the individual molecules inside a loop, we first choose a loop-fixed coordinate system. For definiteness the origin is taken as the molecule nearest to the principal axis that belongs to the largest edge length. In this coordinate system we compute the three-dimensional number density of the molecules, which is then projected onto the best fitting plane. The best fitting plane is defined by the principal axis \vec{n} and passes through the center of mass (COM) of the loop (see Sec. II and inset of Fig. 2). The resulting density for five-, six-, and seven-membered loops [Figs. 3(a)–3(c)] gives an impression of the loop shape. Most importantly, the density distribution in the six-membered loops is strikingly similar to that in a perfect ice crystal [Fig. 3(d)]. This finding shows that clear remnants of the ice structure are still visible in liquid water even at room temperature.

Next we strive to understand how the loops are arranged to form a three-dimensional network. Hence, we calculate the radial distribution function (RDF) of loops in bulk water (Fig. 4). The RDF shows the occurrence of loops of one size as a function of distance. The position of a loop is defined by its center of mass. As loops are not mutually exclusive, a given molecule belongs to many different loops at the same time, meaning in turn that closely neighboring loops will possess a certain number of identical molecules. The solid lines in Fig. 4 present the RDF for the six-membered loops split up according to the number of molecules that are identical with the loop at the origin. A similar calculation can be carried out in the ice crystal leading to the spikes in Fig. 4. Both distributions are remarkably similar with only one major difference in the short-range order: Ice lacks six-membered loops that differ in

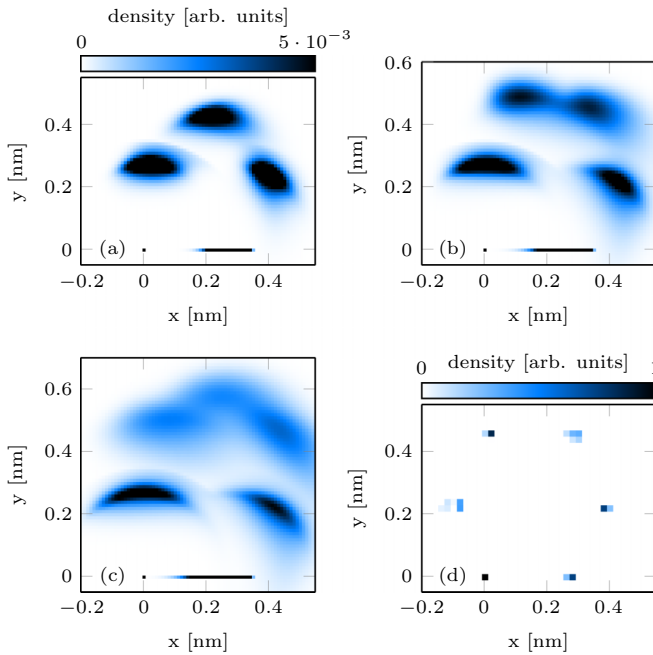


FIG. 3. (Color online) Density distribution of the molecules in (a) five-, (b) six-, and (c) seven-membered loops in liquid water projected on the best fitting plane. In ice Ih the six-membered loops show a sharp hexagonal form (d).

one molecule only, whereas in liquid water about 12% of the six-membered loops have such a close relative (highest peak in Fig. 4).

The findings of this section illustrate that not only the short-range order embodied in the molecular arrangement within the loops but also the long-range order in liquid water still contains certain features reminiscent of the ice crystal structure.

B. Dynamics in bulk water

Experiments and simulations show that hydrogen bonds in water rearrange on the time scale of picoseconds [26,27]. A common way to define the life span of a hydrogen bond from

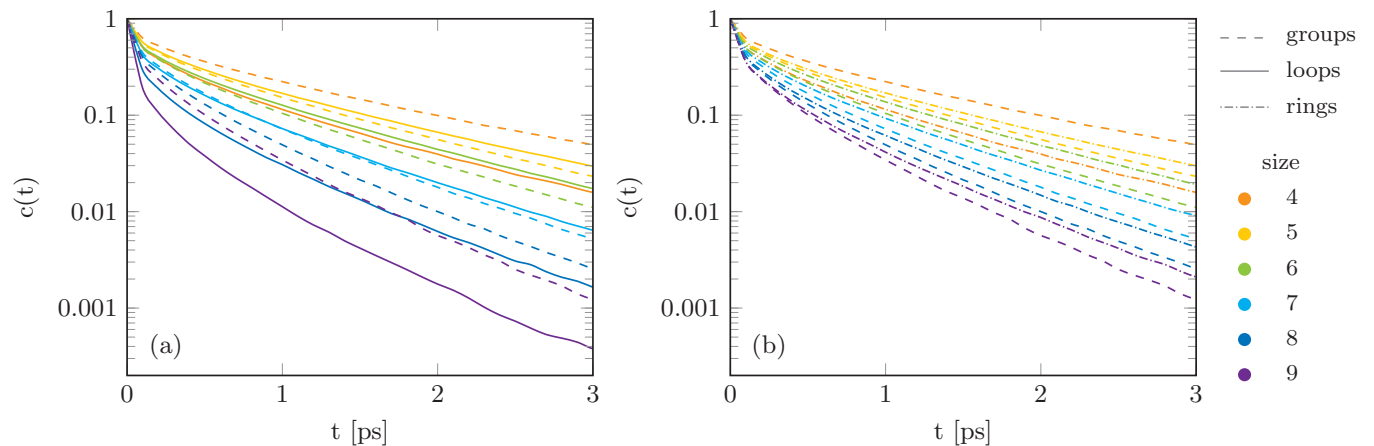


FIG. 5. (Color online) Five- and six-membered loops are stabilized compared to random groups while larger loop sizes are less stable than random groups due to short-circuiting (a). Rings, which are destroyed only due to hydrogen bond breaking and not due to short-circuiting, are stabilized compared to random groups for all ring sizes, except four-membered rings (b).

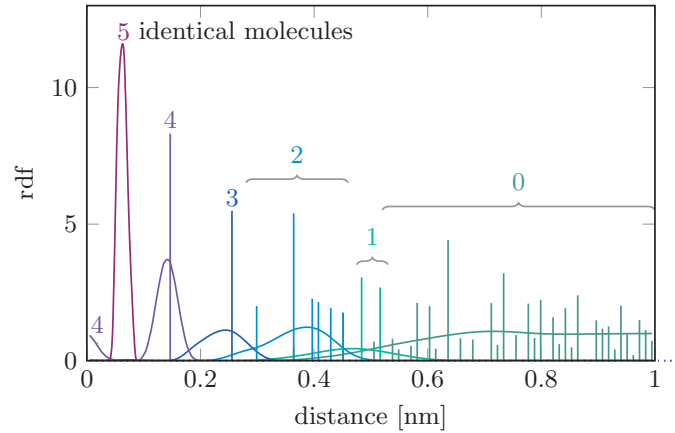


FIG. 4. (Color online) The radial distribution functions of six-membered loops in liquid water and ice (spikes) are remarkably similar. Significant differences occur at very small distances only.

MD simulations is to evaluate the autocorrelation function of the existence operator $h(t)$ [25]:

$$c(t) = \frac{\langle h(0)h(t) \rangle}{\langle h(0) \rangle}. \quad (4)$$

The existence operator $h(t)$ equals one if the hydrogen bond is intact at time t and zero otherwise. The brackets $\langle \rangle$ denote spatial as well as temporal averaging. We apply this framework on the life time of loops of hydrogen bonds. There exist two ways to calculate the correlation function. In the history independent or intermittent life time criterion a loop that existed at $t = 0$ enters the correlation function whenever it exists later, even if it has been broken for some time in between. In the continuous life time criterion a loop which breaks once is regarded broken forever. Here we employ the intermittent life time criterion as it excludes artifacts due to short fluctuations of the bonds that do not lead to a true rearrangement of the network.

Figure 5(a) shows the time-averaged autocorrelation functions for loops of sizes between four and nine members. As a general trend, we expect the life time to be shorter the larger

TABLE I. The average life time $\langle\tau\rangle$ shows that five- and six-membered loops live longer than random groups of the same size, while other loop sizes are more fragile than groups. The faster decay of large loops is related to the formation of short-cuts rather than bond breaking events (see rings and the explanation in the text).

Loop/group size	4	5	6	7	8	9	10
$\langle\tau\rangle$ [ps]							
Groups	0.71	0.49	0.36	0.28	0.22	0.18	0.15
Loops	0.40	0.54	0.42	0.28	0.16	0.09	0.06
Rings	0.40	0.54	0.45	0.33	0.25	0.20	0.16
Loop:group	0.56	1.10	1.15	0.99	0.71	0.51	0.37
Ring:group	0.56	1.11	1.23	1.19	1.11	1.08	1.06

the loop or group becomes as there are more hydrogen bonds that can possibly break. This is indeed observed in Fig. 5(a) with the exception of four-membered loops. Intuitively one might suspect that closing such small rings does not allow optimal binding angles for every participating molecule. Indeed, hydrogen bonds in four-membered loops are less stable than the average hydrogen bond (see Appendix A).

In order to investigate a possible stabilization of certain loop sizes, we compare the decay of random groups that contain a defined number of hydrogen bonds randomly chosen from all existing hydrogen bonds. The number of groups of one size that are chosen at $t = 0$ equals the average number of loops of that size that occur per frame. For the most frequently occurring loop sizes (five- and six-membered loops) we indeed observe a certain stabilization with respect to the random groups. Interestingly, for very small (four) as well as very large (eight, nine) loop sizes the opposite trend is observed.

For a quantitative comparison we strive to calculate the characteristic time scales of the decay processes. Bi- and triexponential fits as well as stretched exponentials have been applied to describe the decay of single hydrogen bonds [29,47]. Librational motion of the molecules is suggested to govern the decay of hydrogen bonds on very short time scales, while rotation and diffusion are associated with the long-time decay [25]. These processes naturally also influence the life time of groups and loops. A triexponential fit is in satisfying agreement with our data (as discussed in Appendix B). Three different time scales have also been identified for the Debye relaxation of water and are suspected to stem from (collective) rearrangements of the hydrogen-bond network [34]. From the fitted functions we calculate the average life time:

$$\langle\tau\rangle = \int_0^{\infty} c(t) dt. \quad (5)$$

The results summarized in Table I support the qualitative conclusions drawn from Fig. 5(a).

One possible reason for the comparatively short life span of large loops is the decay process. Loops are destroyed when one hydrogen bond breaks and also when a shorter connection of hydrogen bonds is formed between two participating molecules, because such a short-circuited ring of hydrogen bonds is no longer regarded a loop. The influence of the different decay processes is tested by counting a loop as intact as long as none of the participating hydrogen

bonds is broken, irrespective of the possible formation of short-cuts [Fig. 5(b) and “ring” in Table I]. Indeed, this additional decay process via short-cuts becomes increasingly important the larger the loop is.

While larger loops were found to be less stable than random groups, rings consistently outlast random groups (with the exception of very small four-membered loops). With increasing size of the rings the difference is diminishing as expected; however, even rings of 10 hydrogen bonds still experience some stabilization. Importantly, the hydrogen bonds involved in a certain ring size are not in general more stable than the average hydrogen bond (see Appendix A, Fig. 13). Hence, the stabilization of rings is clearly a network property which cannot be understood on the level of single hydrogen bonds.

A certain stabilization of hydrogen-bonded clusters is generally expected due to the cooperative character of hydrogen bonds. Interestingly, we observe a stabilization of rings and certain loop sizes even though our MD simulations do not account for these quantum mechanical effects. Including hydrogen-bond cooperativity might enhance the stabilization of rings even more. Further investigations on this topic using methods such as those developed in Ref. [57] for alcohols would provide an interesting subject for future work.

C. Influence of interfaces

Many properties of interfacial water differ greatly from those in bulk [1]. We therefore investigate the influence of interfaces on the hydrogen-bond network. As model surfaces we introduce two diamond sheets confining the water molecules in the z direction (see Sec. II). The origin $z = 0$ is set at the position of the outermost C atoms of one diamond surface. Here we discuss the results gained from the hydrophobic surface only since those for the hydrophilic surface are qualitatively similar and presented in Appendix C.

Control data are collected with “dummy surfaces”: For an undisturbed bulk water simulation we define a virtual plane at an arbitrary position z_p where we cut the box, thus excluding all water molecules behind this virtual plane ($z < z_p$) from the analysis. Consequently, hydrogen bonds that form through the dummy surface are not considered. To ease the comparison to real surfaces the data collected in front of a dummy surface is shifted by the size of the hydrophobic gap so that the first bins containing water coincide.

Water is known to form distinct hydration layers at interfaces. The density profile generally reaches bulk-values at about 1 nm irrespective of the hydrophobicity of the interface (see, e.g., Refs. [54,58]). Similar behavior is observed for our hydrophobic interface (see Fig. 6). Dummy surfaces, on the other hand, are by nature incapable of causing any density fluctuations. Nevertheless, their presence is noticeable in the coordination number, i.e., the number of hydrogen bonds per molecule, which drops near both the dummy and the real surface (Fig. 6). Interestingly, the coordination number near the dummy surface starts to drop significantly earlier than near the real interface. The rearrangement of the molecules manifested in the density fluctuations allows them to maintain the preferred number of binding partners up to the outermost molecules.

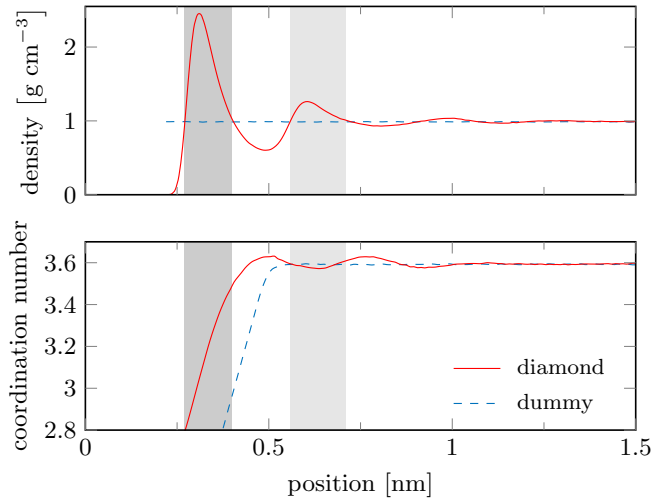


FIG. 6. (Color online) Near real surfaces the water molecules form distinct hydration layers (marked in gray). The coordination number remains almost unchanged except for the outermost molecules. A dummy surface (see text) does not influence the density, but the coordination number starts decreasing at larger distances.

We now evaluate the occurrence of loops as a function of distance to the interface. Every molecule taking part in x loops of size n contributes x/n to the occurrence of this loop size in the molecule's position bin. The average number of loops per molecule is expected to drop at distances where the loops do not fit in arbitrary orientation, i.e., where the distance becomes smaller than the loop size. The results near the dummy surface confirm this expectation (dashed lines in Fig. 7). Near a diamond surface, however, the occurrence of four- to seven-membered loops increases in distance ranges where they are expected to diminish (solid lines and points in Fig. 7). Clearly, the occurrence of loops does not resemble the density fluctuations in a trivial way (note the marked area of the hydration layers).

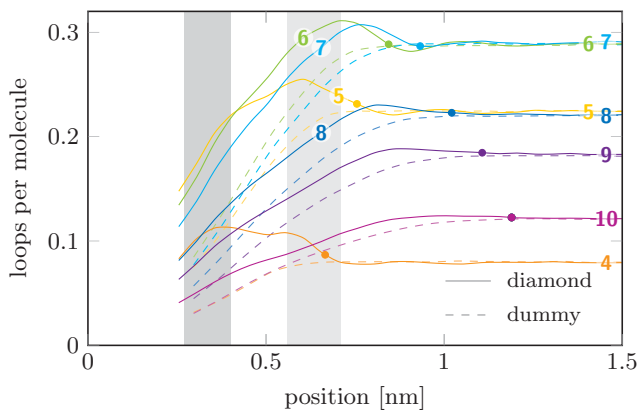


FIG. 7. (Color online) The dashed lines show the occurrence of loops at a dummy surface. At a real diamond interface the occurrence of small loops does not simply drop. The dots mark the minimal distance to the interface at which an average sized loop still fits in arbitrary direction. The positions of the hydration layers are marked in gray (cf. Fig. 6).

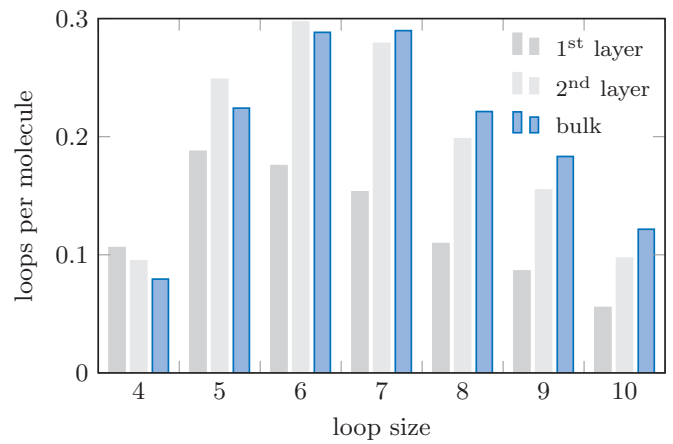


FIG. 8. (Color online) While the occurrence of loops in the second hydration layer resembles that of bulk water, very near to the interface the number of loops per molecule drops and the maximum is shifted to five-membered loops.

Figure 8 shows the average number of loops per molecule evaluated in the hydration layers. While the occurrence of large loops is already decreasing in the second hydration layer, more molecules belonging to smaller loops are found than in the bulk. In the first hydration layer the maximum of the histogram is shifted from six- to five-membered loops. It is an interesting observation that although the coordination number shown in Fig. 6 is dropping in the first hydration layer, smaller loops are favored.

Another topological feature that is influenced by the presence of an interface is the orientation of loops, measured by the scalar product of the normal vector of the loop \vec{n} and the normal vector of the interface \vec{e} (Fig. 9). In bulk $\langle \vec{n} \cdot \vec{e} \rangle = 0.5$ as the loops are randomly arranged. In the very vicinity to the interface only loops that align parallel to the interface remain.

The crosses in Fig. 9 mark the average maximum COM-molecule distance of the loops and show that a reorientation of the loops already happens at distances where they would fit

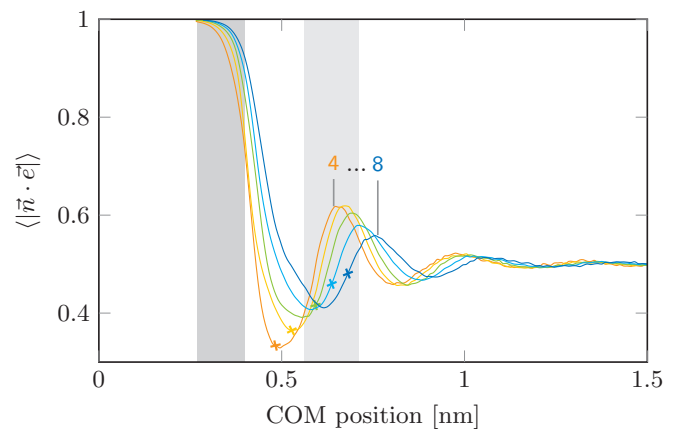


FIG. 9. (Color online) The interface (normal vector \vec{e}) induces a preferred orientation for the loops (normal vector \vec{n}). The crosses mark the average maximum COM-molecule distance of each loop size; i.e., the distance below which the loop does not fit in arbitrary orientations and thus an ordering effect is expected.

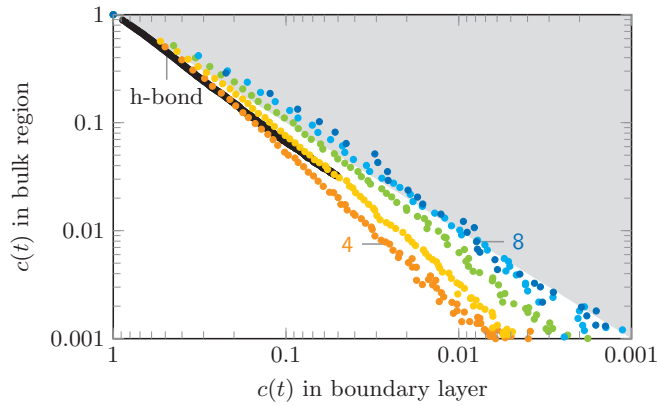


FIG. 10. (Color online) Loop existence autocorrelation function $c(t)$ in bulk water and in the 0.7 nm thick boundary region near hydrophobic model interfaces. Loops in the boundary layer live longer than in the bulk.

in any orientation. This might reflect the density distribution of water near interfaces. The positions of the first hydration layers are marked in gray (cf. Fig. 6). Loops that span the distance between the hydration layers will not lie perfectly parallel to the interface. Therefore, one would expect the average orientation $\langle |\vec{n} \cdot \vec{e}| \rangle$ to drop below the bulk value of 0.5 here. Within a hydration layer one expects to find less loops that lie perpendicular to the interface, because these would reach into the “depletion layer.” The decrease of perpendicular loops might lead to the maxima of $\langle |\vec{n} \cdot \vec{e}| \rangle$. This relationship between the molecular density and the orientation of the loops is supported by four- to six-membered loops with some deviations observed for seven- and eight-membered loops.

To evaluate the influence of an interface on the network dynamics, we calculate the autocorrelation function of loop existence [as defined in Eq. (4)] for a 0.7 nm boundary layer near model interfaces plotted against the same quantity for bulk water (Fig. 10). If the decay in both regions is identical one would expect a line with slope one. Points that lie below this line in the white area of the plot show that the decay in the boundary region is slower than in the bulk. Near the hydrophobic interface the decay of smaller loops is clearly delayed while larger loops seem to be less influenced. This difference most probably comes due to statistics: The larger the loop, the larger is the distance range it spans. This reduces the measurable influence of the interface on the loop. Overall, the decay of loops is affected by interfaces in a similar fashion as that of single hydrogen bonds. The dynamics of water molecules have been found to depend nonmonotonically on the hydrophilicity of the surface [6,9]. At our hydrophilic interface the decay of all loop sizes experiences a significant slow down (see Appendix C, Fig. 19).

D. Loops with the interface

At a hydrophilic interface the water molecules can form hydrogen bonds with polar (partially charged) surface groups. In our case 25% of the terminating surface hydrogen atoms are substituted by hydroxyl groups. When the hydrogen bonds between these OH groups and water are considered part of the network, we count significantly more loops in the

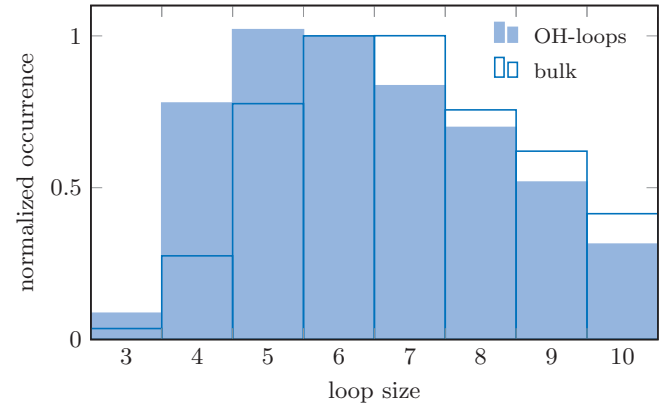


FIG. 11. (Color online) The occurrence of loops per OH group of the interface (filled boxes) is shifted to smaller loop sizes compared to loops per water molecule in bulk water (dark border; cf. Fig. 2). The results are normalized to the occurrence of six-membered loops.

boundary region (see Appendix C, Fig. 16 and 17). Small loops containing OH groups are clearly favored. This becomes apparent from Fig. 11, where the number of loops per OH group is compared to the number of loops per water molecule in bulk (cf. Fig. 2). The results are normalized to the occurrence of six-membered loops and indicate a shift to smaller loop sizes including OH groups.

Considering the dynamics, loops formed with the interface clearly outlive the pure water loops found within the boundary region of 0.7 nm (Fig. 12). This enhanced life span can be explained by the close vicinity of the OH loops to the interface where the slowing influence on the dynamics of the water molecules is strongest. Additionally, surface OH groups are immobile and thus cannot diffuse away leading to a reduction of possible breaking points in the loop.

Another interesting feature of the OH loops is that their stability strictly decreases with increasing size, in contrast to bulk water loops where four-membered loops are unexpectedly short lived. The destabilization of the hydrogen bonds in such small loops due to unfavorable angular restraints seems to be compensated when OH groups serve as binding partners.

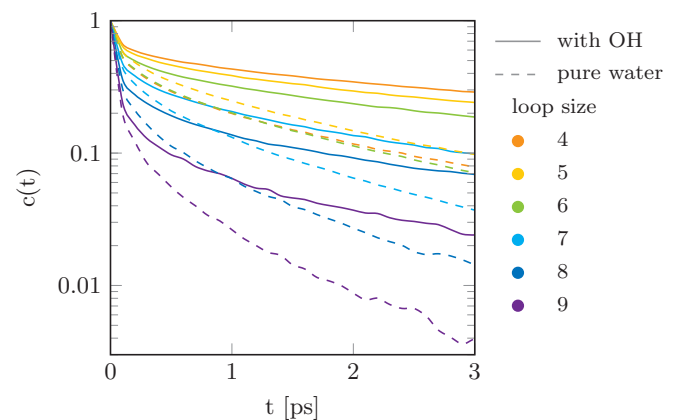


FIG. 12. (Color online) Loops that contain at least one OH group of the interface are significantly more stable than the pure water loops that are found in the 0.7 nm thick boundary region (dashed lines).

E. Connection to single-molecule investigations

Interfacial water from the viewpoint of a single molecule has been intensively studied recently, and we now connect our results to some earlier works. The orientation of single molecules has been found to follow a well-defined pattern near hydrophobic interfaces with the aim of reducing as much as possible the number of dangling bonds [8,15,32,53,59]. Apparently this goal can best be accomplished by forming smaller loops near the interface as borne out by the loop size distribution shown in Fig. 8. At a hydrophilic interface a similar effect is observed for bonds including interfacial OH groups in Fig. 11. The prolonged life time of loops near interfaces in the hydrophobic (Fig. 10) and hydrophilic (Figs. 12 and 19) interfaces clearly corresponds with the enhanced stability of hydrogen bonds and generally slower water dynamics [4,9,12,28,30,60–64], which has often been explained by excluded volume effects in the context of the jump mechanism for hydrogen-bond exchange.

The most prominent examples for the importance of collective effects in water are its dielectric properties. The changes in network characteristics due to the presence of an interface as observed in the present work are clearly mirrored in the strongly varying and highly anisotropic dielectric properties of interfacial water [37–40,44,55,65–69]. The relation between water’s network structure and its dielectric properties is, however, far from trivial even for bulk water and represents an interesting field for future investigations. This is reiterated by recent findings in alcohols [57] where clear evidence for the presence of supramolecular structures was presented, but only some of them (globules) were found to contribute to the famous Debye process in dielectric relaxation spectra, whereas others (transient chains) did not.

IV. CONCLUSION

Liquid water forms a transient network composed of loops which are closed, non-short-circuited paths of molecules connected by hydrogen bonds. We showed that these loops are mostly planar. By projecting the molecule densities on the best fitting plane we found that the loop shape in liquid water and ice Ih is surprisingly similar. Even the long-range order embodied in the radial distribution function of loops is strikingly similar for six-membered loops in liquid water and ice.

Loops of five to seven molecules are known to dominate the hydrogen-bond network of liquid water. Indeed, we find that loops of at least five molecules stay intact as closed rings for a significantly longer period than random groups of the same size. The difference is decreasing with increasing ring size, but the stabilization of rings is still clearly visible even for 10-membered rings.

At interfaces the number of loops with fewer than eight hydrogen bonds increases in a distance range where it would naively be expected to diminish. The maximum of the distribution is shifted to five-membered loops in the first hydration layer. The observed changes in the network topology do not reflect the density distribution in a trivial way and are not expected from the coordination number. The decay of loops slows down near interfaces in accordance with the prolonged

life time of the hydrogen bonds. We find extraordinarily stable loops formed between OH groups of the hydrophilic diamond surface and adjacent water molecules. These OH loops clearly outlive the nearby pure water loops.

ACKNOWLEDGMENTS

The authors gratefully acknowledge funding from the Volkswagen Foundation and the Deutsche Forschungsgemeinschaft Graduiertenkolleg 1640. Computing time has been granted by the John von Neumann Institute for Computing (NIC) and provided on the supercomputer JUROPA at Jülich Supercomputing Centre (JSC).

APPENDIX A: STABILIZATION AS A TRUE NETWORK CHARACTERISTIC

The stabilization found for loops of five and six hydrogen bonds might be explained from the viewpoint of single hydrogen bonds: If optimal binding angles lead to rings of five or six molecules, one would expect that these loops contain the most stable hydrogen bonds. Then any hydrogen bond participating in such a loop is expected to decay more slowly than the average hydrogen bond. However, this is not supported by our data (Fig. 13). Here we compare the autocorrelation function $c(t)$ [Eq. (4)] of single hydrogen bonds that are part of at least one n -membered loop at $t = 0$ ($n = 4, \dots, 9$) to the decay averaged over all existing hydrogen bonds. The decay of single hydrogen bonds participating in loops is found to be identical to the decay of any arbitrary hydrogen bond. Thus, the observed stabilization of five- and six-membered loops does not stem from an overall stabilization of hydrogen bonds in these loops but is suggested to reveal an underlying enhanced correlation of hydrogen bonds within loops.

The only case where we find a small deviation is four-membered loops. Hydrogen bonds of four-membered loops decay slightly faster than the average hydrogen bond. The comparably fast decay of four-membered loops can thus be

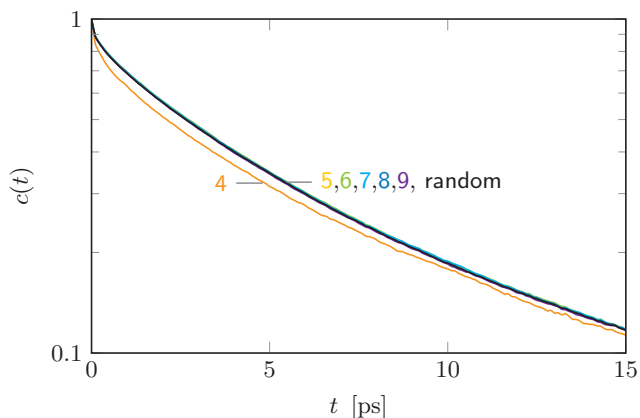


FIG. 13. (Color online) The congruency of the correlation functions of random hydrogen bonds and those participating in loops shows that the stabilization of certain loop sizes does not stem from a stabilization of the hydrogen bonds themselves. An exception are hydrogen bonds in four-membered loops that show to be less stable than the average hydrogen bond.

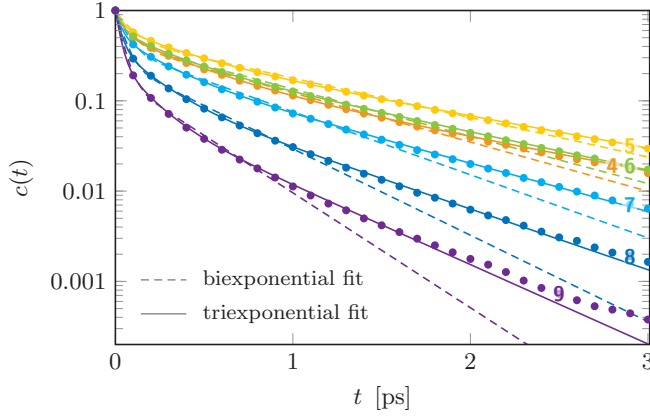


FIG. 14. (Color online) The autocorrelation functions $c(t)$ (here shown for loops of four to nine hydrogen bonds) are well described by triexponential fits (solid lines), while biexponential fitting is clearly insufficient (dashed lines).

explained by the generally reduced stability of the contributing bonds.

APPENDIX B: FITTING THE DECAY OF HYDROGEN-BONDED LOOPS AND GROUPS

The decay of groups and loops of hydrogen bonds is clearly suggesting the existence of more than one characteristic time scale. Following previous work on the decay of single hydrogen bonds [47], we fit the dynamics with the assumption of two and three time scales (Fig. 14). The triexponential fit

$$c(t) = a_1 e^{-\frac{t}{\tau_1}} + a_2 e^{-\frac{t}{\tau_2}} + a_3 e^{-\frac{t}{\tau_3}} \quad (\text{B1})$$

with the parameters shown in Table II is found to match well and is used to calculate the average life time [Eq. (5)]:

$$\langle \tau \rangle = a_1 \cdot \tau_1 + a_2 \cdot \tau_2 + a_3 \cdot \tau_3. \quad (\text{B2})$$

As for single hydrogen bonds, it is difficult to assign the different time scales to particular physical processes. The decay dynamics of hydrogen bonds are commonly associated with librational motion of the molecules on short time scales and rotation and diffusion on longer time scales. Combining these mechanisms into one average life time allows the comparison of the decay of different loop sizes, groups, and rings at a glance (Table I).

TABLE II. Results of the triexponential fit [Eq. (B1)] for loops.

Loop size	4	5	6	7	8	9	10
a_1	0.44	0.36	0.39	0.47	0.61	0.71	0.80
τ_1 [ps]	0.04	0.04	0.04	0.03	0.03	0.03	0.02
a_2	0.34	0.30	0.29	0.29	0.25	0.20	0.16
τ_2 [ps]	0.36	0.34	0.28	0.23	0.19	0.14	0.12
a_3	0.22	0.34	0.32	0.24	0.14	0.09	0.04
τ_3 [ps]	1.17	1.23	1.03	0.81	0.65	0.49	0.43

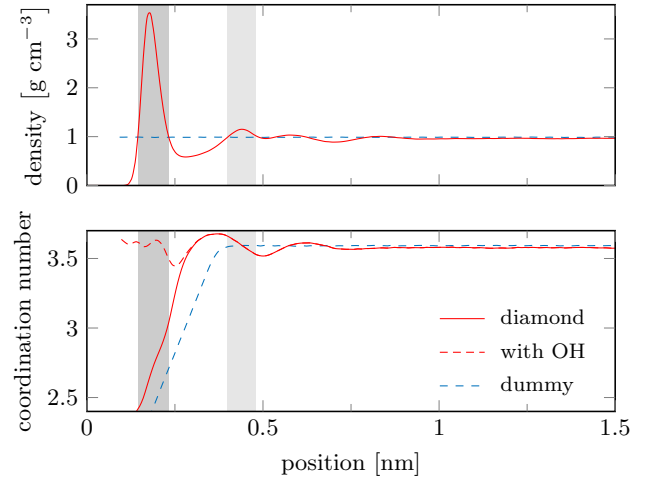


FIG. 15. (Color online) Density and coordination number near the hydrophilic interface and dummy surface (cf. Fig. 6). The outermost molecules manage to maintain the favored number of hydrogen bonds by binding to OH groups (dashed red line). The positions of the hydration layers are marked in gray.

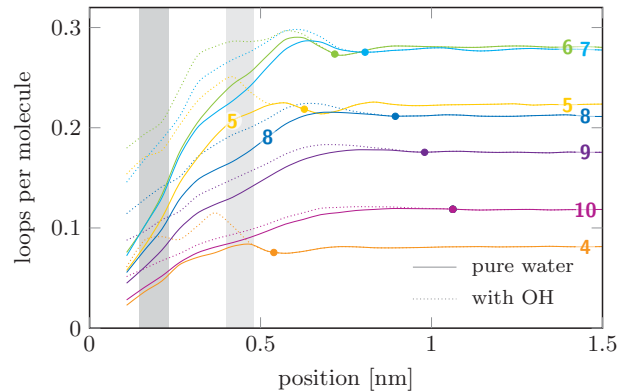


FIG. 16. (Color online) The occurrence of loops at a hydrophilic surface shows a very similar behavior as observed at the hydrophobic interface. Including hydrogen bonds with OH groups increases the number of loops near the interface (dashed lines). The gray areas indicate the position of the density maxima (cf. Fig. 15).

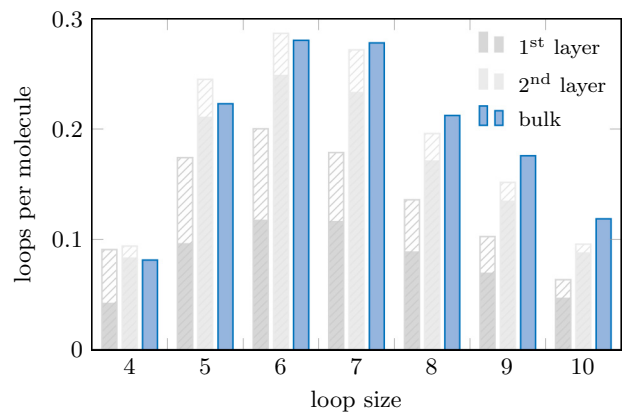


FIG. 17. (Color online) The number of loops decreases the nearer the interface is. The maximum remains at six-membered loops. The number of loops increases by the striped part of the boxes, when OH groups are considered valid members of the hydrogen bond network.

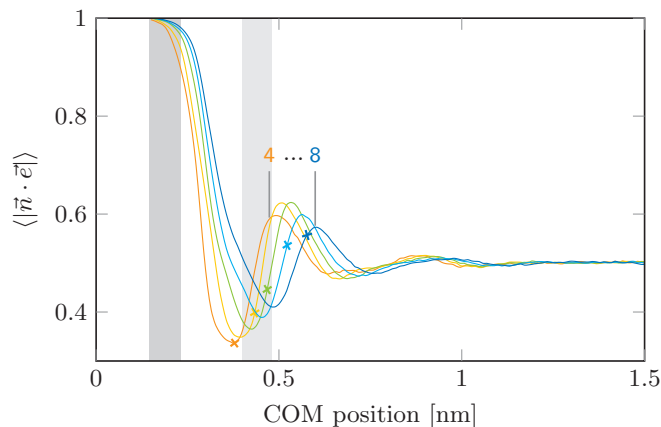


FIG. 18. (Color online) The hydrophilic interface (normal vector \vec{e}) induces a preferred orientation for the loops (normal vector \vec{n}). The crosses mark the distance below which loops do not fit in arbitrary orientation (cf. Fig. 9).

APPENDIX C: HYDROPHILIC BOUNDARY

As a comparison to the data discussed at a hydrophobic surface (Sec. III C), the corresponding plots for the hydrophilic surface are shown here. The hydrophilic surface provides OH groups as binding partners. Considering them valid members of the hydrogen bond network influences the topology.

The density and coordination number fluctuations are more pronounced at the hydrophilic surface (Fig. 15) than at the hydrophobic one (Fig. 6). When including the hydrogen bonds that are formed with OH groups, the favored coordination number is recovered in the first hydration shell (dashed red line in Fig. 15).

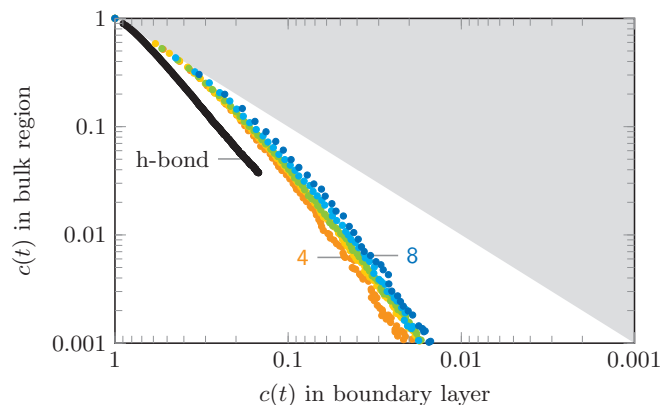


FIG. 19. (Color online) The life time of loops in the 0.7 nm boundary region is significantly longer than in the bulk.

The occurrence of loops (Fig. 16) looks very similar to that observed at the hydrophobic interface (Fig. 7). The number of four- to seven-membered loops increases in distance ranges where they are expected to diminish. Unlike the hydrophobic surface, the most frequently occurring loop sizes remain six and seven for all distance ranges. The histogram of the occurrence of loops in the hydration layers and bulk confirms this (Fig. 17). The hydrogen bonds formed with OH groups lead to a higher number of loops of all sizes near the boundary. Small loops are affected more significantly. The orientation of loops near the hydrophilic surface is influenced in a very similar way as observed at the hydrophobic surface (Fig. 18 and Fig. 9, respectively).

The slowdown of the dynamics in the 0.7 nm boundary region is more pronounced for the hydrophilic surface (Fig. 19) than for the hydrophobic one (Fig. 10).

- [1] P. Ball, *Chem. Rev.* **108**, 74 (2008).
- [2] P. Ball, *Nature (London)* **478**, 467 (2011).
- [3] S. H. Lee and P. J. Rossky, *J. Chem. Phys.* **100**, 3334 (1994).
- [4] D. Argyris, T. Ho, D. R. Cole, and A. Striolo, *J. Phys. Chem. C* **115**, 2038 (2011).
- [5] Y. von Hansen, S. Gekle, and R. R. Netz, *Phys. Rev. Lett.* **111**, 118103 (2013).
- [6] S. Romero-Vargas Castrillón, N. Giovambattista, I. A. Aksay, and P. G. Debenedetti, *J. Phys. Chem. B* **113**, 1438 (2009).
- [7] M. Ji, M. Odellius, and K. J. Gaffney, *Science* **328**, 1003 (2010).
- [8] G. Stirnemann, P. J. Rossky, J. T. Hynes, and D. Laage, *Faraday Discuss.* **146**, 263 (2010).
- [9] G. Stirnemann, S. R.-V. Castrillón, J. T. Hynes, P. J. Rossky, P. G. Debenedetti, and D. Laage, *Phys. Chem. Chem. Phys.* **13**, 19911 (2011).
- [10] D. Laage, G. Stirnemann, F. Sterpone, R. Rey, and J. T. Hynes, *Annu. Rev. Phys. Chem.* **62**, 395 (2011).
- [11] D. Laage, G. Stirnemann, F. Sterpone, and J. T. Hynes, *Acc. Chem. Res.* **45**, 53 (2012).
- [12] G. Stirnemann, E. Wernersson, P. Jungwirth, and D. Laage, *J. Am. Chem. Soc.* **135**, 11824 (2013).
- [13] K. Mazur, R. Buchner, M. Bonn, and J. Hunger, *Macromolecules* **47**, 771 (2014).
- [14] M. Bonn, Y. Nagata, and E. H. G. Backus, *Angew. Chem.* **127**, 5652 (2015).
- [15] N. Giovambattista, P. J. Rossky, and P. G. Debenedetti, *Phys. Rev. E* **73**, 041604 (2006).
- [16] M. Bonn, H. J. Bakker, Y. Tong, and E. H. G. Backus, *Biointerphases* **7**, 20 (2012).
- [17] K. Shiraga, T. Suzuki, N. Kondo, and Y. Ogawa, *J. Chem. Phys.* **141**, 235103 (2014).
- [18] S. Strazdaite, J. Versluis, E. H. G. Backus, and H. J. Bakker, *J. Chem. Phys.* **140**, 054711 (2014).
- [19] D. L. Bergman, *Chem. Phys.* **253**, 267 (2000).
- [20] M. Matsumoto, *J. Chem. Phys.* **126**, 054503 (2007).
- [21] R. H. Henschman and S. J. Irudayam, *J. Phys. Chem. B* **114**, 16792 (2010).
- [22] E. Arunan, G. R. Desiraju, R. A. Klein, J. Sadlej, S. Scheiner, I. Alkorta, D. C. Clary, R. H. Crabtree, J. J. Dannenberg, P. Hobza, H. G. Kjaergaard, A. C. Legon, B. Mennucci, and D. J. Nesbitt, *Pure Appl. Chem.* **83**, 1637 (2011).
- [23] D. Prada-Gracia, R. Shevchuk, and F. Rao, *J. Chem. Phys.* **139**, 084501 (2013).
- [24] A. Ozkanlar, T. Zhou, and A. E. Clark, *J. Chem. Phys.* **141**, 214107 (2014).
- [25] A. Luzar and D. Chandler, *Phys. Rev. Lett.* **76**, 928 (1996).
- [26] C. J. Fecko, *Science* **301**, 1698 (2003).

- [27] K. A. Tay and F. Bresme, *Phys. Chem. Chem. Phys.* **11**, 409 (2009).
- [28] A. A. Bakulin, M. S. Pshenichnikov, H. J. Bakker, and C. Petersen, *J. Phys. Chem. A* **115**, 1821 (2011).
- [29] F. W. Starr, J. K. Nielsen, and H. E. Stanley, *Phys. Rev. E* **62**, 579 (2000).
- [30] M. Rosenstihl, K. Kämpf, F. Klameth, M. Sattig, and M. Vogel, *J. Non-Cryst. Solids* **407**, 449 (2015).
- [31] F. Klameth and M. Vogel, *J. Chem. Phys.* **138**, 134503 (2013).
- [32] M. F. Harrach, F. Klameth, B. Drossel, and M. Vogel, *J. Chem. Phys.* **142**, 034703 (2015).
- [33] M. Sharma, R. Resta, and R. Car, *Phys. Rev. Lett.* **98**, 247401 (2007).
- [34] A. Beneduci, *J. Mol. Liq.* **138**, 55 (2008).
- [35] M. Heyden, J. Sun, S. Funkner, G. Mathias, H. Forbert, M. Havenith, and D. Marx, *Proc. Natl. Acad. Sci. USA* **107**, 12068 (2010).
- [36] A. Y. Zasetsky, *Phys. Rev. Lett.* **107**, 117601 (2011).
- [37] D. J. Bonthuis, S. Gekle, and R. R. Netz, *Phys. Rev. Lett.* **107**, 166102 (2011).
- [38] S. Gekle and R. R. Netz, *J. Chem. Phys.* **137**, 104704 (2012).
- [39] C. Zhang, F. Gygi, and G. Galli, *J. Phys. Chem. Lett.* **4**, 2477 (2013).
- [40] S. Gekle and R. R. Netz, *J. Phys. Chem. B* **118**, 4963 (2014).
- [41] M. Sajadi, F. Berndt, C. Richter, M. Gerecke, R. Mahrwald, and N. P. Ernsting, *J. Phys. Chem. Lett.* **5**, 1845 (2014).
- [42] P. A. Bopp, A. A. Kornyshev, and G. Sutmann, *Phys. Rev. Lett.* **76**, 1280 (1996).
- [43] B. Sahin and B. Ralf, *J. Phys.: Condens. Matter* **26**, 285101 (2014).
- [44] C. Schaaf and S. Gekle, *Phys. Rev. E* **92**, 032718 (2015).
- [45] A. Rahman and F. H. Stillinger, *J. Am. Chem. Soc.* **95**, 7943 (1973).
- [46] D. Rapaport, *Mol. Phys.* **50**, 1151 (1983).
- [47] A. C. Belch and S. A. Rice, *J. Chem. Phys.* **86**, 5676 (1987).
- [48] H. J. C. Berendsen, J. R. Grigera, and T. P. Straatsma, *J. Phys. Chem.* **91**, 6269 (1987).
- [49] S. Pronk, S. Pall, R. Schulz, P. Larsson, P. Bjelkmar, R. Apostolov, M. R. Shirts, J. C. Smith, P. M. Kasson, D. van der Spoel, B. Hess, and E. Lindahl, *Bioinformatics* **29**, 845 (2013).
- [50] C. Oostenbrink, A. Villa, A. E. Mark, and W. F. Van Gunsteren, *J. Comput. Chem.* **25**, 1656 (2004).
- [51] U. Essmann, L. Perera, M. L. Berkowitz, T. Darden, H. Lee, and L. G. Pedersen, *J. Chem. Phys.* **103**, 8577 (1995).
- [52] S. Miyamoto and P. A. Kollman, *J. Comput. Chem.* **13**, 952 (1992).
- [53] F. Sedlmeier, J. Janecek, C. Sendner, L. Bocquet, R. R. Netz, and D. Horinek, *Biointerphases* **3**, FC23 (2008).
- [54] C. Sendner, D. Horinek, L. Bocquet, and R. R. Netz, *Langmuir* **25**, 10768 (2009).
- [55] D. J. Bonthuis, S. Gekle, and R. R. Netz, *Langmuir* **28**, 7679 (2012).
- [56] W. H. Press (ed.), *Numerical Recipes in C: The Art of Scientific Computing*, 2nd ed. (Cambridge University Press, Cambridge, 1992).
- [57] P. Wieth and M. Vogel, *J. Chem. Phys.* **140**, 144507 (2014).
- [58] A. Striolo, *Adsorption Sci. Tech.* **29**, 211 (2011).
- [59] P. N. Perera, K. R. Fega, C. Lawrence, E. J. Sundstrom, J. Tomlinson-Phillips, and D. Ben-Amotz, *Proc. Natl. Acad. Sci. USA* **106**, 12230 (2009).
- [60] D. Laage, G. Stirnemann, and J. T. Hynes, *J. Phys. Chem. B* **113**, 2428 (2009).
- [61] K. J. Tielrooij, N. Garcia-Araez, M. Bonn, and H. J. Bakker, *Science* **328**, 1006 (2010).
- [62] K. J. Tielrooij, S. T. van der Post, J. Hunger, M. Bonn, and H. J. Bakker, *J. Phys. Chem. B* **115**, 12638 (2011).
- [63] M. D. Fayer, *Acc. Chem. Res.* **45**, 3 (2012).
- [64] N. Galamba, *J. Phys. Chem. B* **118**, 4169 (2014).
- [65] M. Ahmad, W. Gu, T. Geyer, and V. Helms, *Nat. Commun.* **2**, 261 (2011).
- [66] M. Heyden, D. J. Tobias, and D. V. Matyushov, *J. Chem. Phys.* **137**, 235103 (2012).
- [67] S. Parez, M. Předota, and M. Machesky, *J. Phys. Chem. C* **118**, 4818 (2014).
- [68] K. F. Rinne, S. Gekle, and R. R. Netz, *J. Phys. Chem. A* **118**, 11667 (2014).
- [69] K. F. Rinne, S. Gekle, and R. R. Netz, *J. Chem. Phys.* **141**, 214502 (2014).